J Fluoresc (2006) 16:461–468
DOI 10.1007/s10895-006-0085-9

ORIGINAL PAPER

Er, Yb Doped Yttrium Based Nanosized Phosphors: Particle Size, "Host Lattice" and Doping Ion Concentration Effects on Upconversion Efficiency

Ana Maria Pires · Stephan Heer · Hans Ulrich Güdel · Osvaldo Antonio Serra

Received: 3 November 2005 / Accepted: 21 February 2006 / Published online: 16 May 2006

Abstract The upconverter phosphors studied herein have different percentages of Er^{3+} and Yb^{3+} as doping ions in different Y^{3+} matrixes (Y_2O_3, Y_2O_2S), and were prepared from different precursors (polymeric resin, oxalate, basic carbonate) and method (combustion). Upconversion emission spectra were recorded at 298 K for all the doped samples in the visible region, for efficiency and Green/Red emission relative intensity comparisons. Therefore, an investigation of the influence of the doping ion concentration, particle size and host lattice on the upconversion process is provided in view of the UPT (Upconverting phosphor technology application). On the basis of the results, it was possible to evaluate the best combination for a specific assay, considering whether it is advantageous to have the greatest contribution from the green or red emissions, or from both in comparable intensities.

Keywords Upconversion · Rare earth · Phosphor · UPT · Nanoparticles.

Introduction

UPT (Upconverting phosphor technology) involves the detection of analytes by immunoassay [1–2] and is based on lanthanide-containing, submicrometer-sized, ceramic particles that can absorb infrared light and emit visible light. For this specific application, the desired phosphor upconverter must have morphological and optical features that are suitable for a good conjugation with biological metabolites, as well as exhibit high intensity emission, leading to a detectable signal. In a previous paper, we reported luminescent and morphological studies of yttrium oxide samples doped with ytterbium and erbium prepared by either the combustion method, Pechini's method, or the thermal decomposition of oxalate or basic carbonate precursors, in order to investigate appropriate systems for UPT [3]. Concerning the application in the UPT field in particular, it was demonstrated that the polymeric and basic carbonate precursors lead to spheroidal powder particles that are more suitable for immunoassays. In addition, spectroscopic data obtained at room temperature indicated that nanosized yttrium oxide with a percentage of Yb^{3+} 40 times higher than that of Er^{3+} has an additional enhancement in Er^{3+} red emission. A significant enhancement in the red upconverted emission at room temperature was also observed in Y_2O_3:Yb^{3+}, Er^{3+} prepared by the combustion method, and the magnitude of the emission was related to the concentration of Yb^{3+} ions [4]. In addition, a detailed report providing low temperature upconversion spectroscopy of nanosized Y_2O_3:Er(2%),Yb(1%) phosphor from polymeric precursor was also recently published [5].

The upconverter nanophosphors studied in the present work contain Er^{3+} and Yb^{3+} as doping ions in a Y^{3+} matrix prepared from the polymeric resin and basic carbonate precursors. Bulk oxide samples were also obtained from the oxalate precursor so that a comparison between these samples and the nanosized ones could be made [3, 6]. Factors like the doping ion concentration, particle size, and host lattice must play an important role and influence the upconversion process. Therefore, upconversion emission spectra were

A. Pires · O. A. Serra (✉)
Departamento de Química, FFCLRP, Universidade de São Paulo,
Av. Bandeirantes 3900,
14040-901 Ribeirão Preto, SP, Brazil
e-mail: osaserra@usp.br.

S. Heer · H. U. Güdel
Department of Chemistry and Biochemistry, University of Bern,
Freiestrasse 3,
3000 Berne 9, Switzerland

recorded in a suitable geometry, at room temperature, for the doped yttrium oxide and oxysulfide in the visible region, for comparison of the efficiencies and Green/Red emission relative intensities.

Experimental

Sample preparation

Yttrium, ytterbium, and erbium oxides (99.99%) were used as starting materials. Other chemicals used were reagent grade. The yttrium oxide samples doped with ytterbium and erbium were prepared by the thermal decomposition (750°C, 4 hr) of either basic carbonate or polymeric and oxalate precursors, as well as from the combustion method [3]. The yttrium oxysulfide doped samples were prepared as described elsewhere [6], by using the reaction between sulfur vapor and polymeric resin or basic carbonate.

Structural and morphological characterization

X-ray diffractometry, XRD (SIEMENS D5000 diffractometer, K_α Cu radiation, $\lambda = 1.5418$ Å, graphite monochromator); transmission electron microscopy, TEM (Philips CM200 transmission microscope, equipped with Digital Spectrometer – Prism PGT – Princeton Gamma Tech); and scanning electron microscopy, SEM (JSM-5900LV or ZEISS DSM 940A microscopes) were performed for structural and morphological characterization.

Spectroscopic setup

Continuous-wave excitation measurements at 298 K were performed for the samples placed in a standard tubing holder, at a fixed geometry, by using the following set-up: luminescence was excited with a tunable CW Ti:sapphire laser (Spectra Physics) pumped by an Ar-laser (Spectra Physics 2045-15); the excitation energy position was optimized by eye, and details about incident power and beam size as well as excitation energy positions are given in the appropriate figure captions. VIS luminescence was collected by a fiber flame resistant probe and recorded by a Fiberspectrometer (HR2000CG-UV-NIR) system. All spectra were corrected using an LS1 tungsten halogen lamp as reference, as well as the subtraction of the dark spectrum measured in the same conditions.

Results and discussion

Structural and morphological characterization

All the obtained samples were characterized by XRD, part of this characterization had been reported before [3], confirming that the thermal treatment of the precursors at 750°C, 4 hr, under static air resulted in the body-centered cubic structure of the Y_2O_3 crystalline phase (PDF No. 43-1036) with spatial group *Ia3*, in which Y^{3+} occupies a unit cell that has three sites with point-group symmetry C_2 and one with point-group symmetry $C_{3i} \equiv S_6$ with an inversion center [7, 8].

On the other hand, samples prepared by the reaction between precursors and sulfur vapor resulted in diffraction patterns typical of Y_2O_2S, trigonal space group P3 ml (D_{3d}^3), as previously reported [6], where both Y and O atoms have the same symmetry site, C_{3v}. Each metal atom Y is coordinated to four oxygen atoms and three sulfur atoms as its nearest neighbor. This is a rare seven-coordinated geometry where four Y atoms tetrahedrally coordinate around one oxygen atom. The S site is octahedrally coordinated by six Y atoms, having symmetry D_{3d}. Further observation of the structure revealed that Y-atom planes, O-atom planes, and S-atom planes are all perpendicular to the c axis of the trigonal crystal. This characteristic uniaxial structure may cause anisotropy in some physical properties such as lattice vibration modes or dielectric tensor components [9].

Particle shape and size were evaluated by the TEM and SEM techniques; some of the data had already been published [3, 6]. Figure 1 shows TEM representative images for several samples. The doping ion concentration, the precursor employed, and host lattice were varied and had been not reported before. Table 1 summarizes the main features of each produced sample, such as crystalline phase, employed precursor, particle size and shape, and doping ion percentage, in order to facilitate comparisons between them.

Spectroscopic measurements

The investigated upconverter phosphor contains Er^{3+} and Yb^{3+} as doping ions. The infrared quanta near 980 nm are absorbed by Yb^{3+} ions, and then the energy is transferred to the activator (Er^{3+}) ions in a two-step energy transfer (ET). This is the usual mechanism in such systems. However, factors like the doping ion concentration, particle size, and host lattice must play an important role and thus influence the upconversion process.

The emission spectra at 298 K in the visible region (green and red) corresponding to some of the synthesized doped yttrium based phosphors are shown in Fig. 2i. It is possible to observe upconversion emission in the green, $^2H_{11/2}$, $^4S_{3/2} \rightarrow {}^4I_{15/2}$, and red, $^4F_{9/2} \rightarrow {}^4I_{15/2}$, regions for all the phosphors, independent of the matrix and doping ion concentration. The relative intensity was evaluated from comparison of the maximum intensity of the observed transition in each spectral region (green and red), and is represented in the graph shown in Fig. 2ii. It is possible to verify that the doping ion percentage plays the most important role in the relative

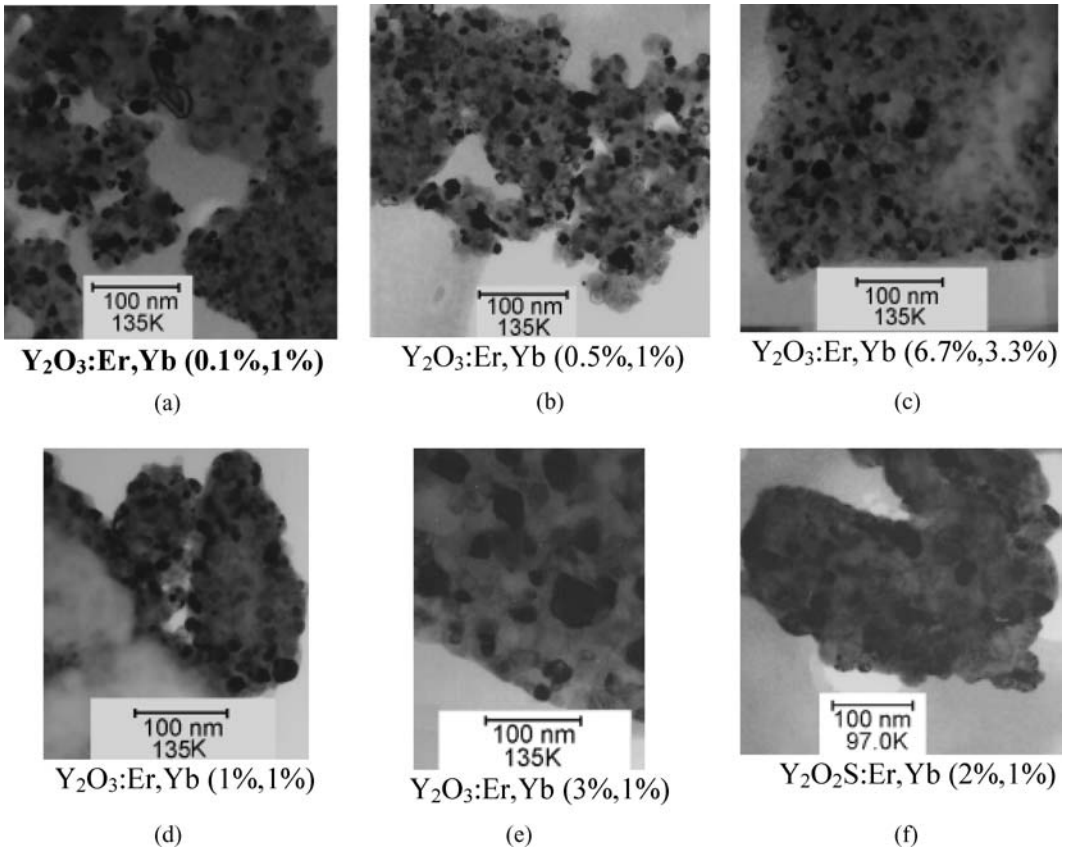

Fig. 1 TEM dark field images under 200 kV for Er–Yb doped Y_2O_3 and Y_2O_2S samples with different doping ion content, prepared from the polymeric precursor

intensity of the studied phosphors. When the percentage of Yb is increased, the red contribution is enhanced, in agreement with the work previously reported [3]. The influence of particle size can be checked by comparing samples with the same lattice and percentage of Er,Yb, but prepared from different precursors; i.e., Y_2O_2S:Er,Yb (0.1%,4%) obtained from basic carbonate and Y_2O_2S:Er,Yb (0.1%,4%) obtained from polymeric resin, as described in Table 1. In this case, the same green/red relative intensity ratio is observed, indicating that the use of both types of precursors does not lead to measurable differences between the red and green emission ratio. The standard bulk oxysulfide data were included to show that, even in the presence of lanthanum instead of yttrium as the host lattice cation, the red contribution is higher than the green one, as in our prepared cases, even though the green emission of the standard bulk oxysulfide has a smaller percentage than of Y_2O_2S:Er,Yb (2%,1%) prepared from the polymeric resin.

In order to compare the upconversion efficiency in terms of number of photons produced by the different oxysulfide samples, it was plotted the number of photons on the *y*-axis v. wavenumbers on the *x*-axis, whereas the relationship between photon counts and intensity is as follows: photon counts of a band = intensity of the band multiplied by wavelength. Then, the photon ratio between green and red regions were also evaluated for the spectrum of each sample, taking into account that all the spectra were measured in the same geometry and with the same scanning parameters, such as integration time and number of averaging scans. So, in Fig. 3, a comparison between Y_2O_2S:Er,Yb (0.1%,4%) obtained from basic carbonate, Y_2O_2S:Er,Yb (0.1%,4%) and Y_2O_2S:Er,Yb (2%,1%), both obtained from polymeric resin, is plotted. By analyzing Fig. 3, it is possible to confirm that the most efficient phosphors are the ones prepared from polymeric resin, considering that the one with 0.1% of Er^{3+} and 0.4% of Yb^{3+} being the most intense. Therefore, Y_2O_2S:Er,Yb (0.1%,4%) phosphor prepared from the polymeric resin is more efficient than the Y_2O_2S:Er,Yb (0.1%,4%) one prepared from basic carbonate, although these two samples present almost the same red and green relative intensities according to Fig. 2.ii. It is interesting to note that the Y_2O_2S:Er,Yb (2%,1%) obtained from polymeric resin exhibits the strongest green emission, indicating that a decreasing in the content of Yb and an increase in the percentage of Er do not strongly diminish the photon ratio when compared to the other samples, but enhance the upconversion process in the green region.

Table 1 Upconverter phosphor samples characterized by upconversion luminescence techniques

Host lattice	Precursor	Crystalline phase	Er (%)	Yb (%)	Particle size (nm)	Particle shape
Y_2O_3	Polymeric resin	Cubic-Y_2O_3	0.5	6.6	Aggregates of 10–20	Spheroidal
Y_2O_3	Polymeric resin	Cubic-Y_2O_3	0.1	4.0	Aggregates 10–20	Spheroidal
Y_2O_3	Basic carbonate	Cubic-Y_2O_3	0.1	4.0	~90	Spherical
Y_2O_3	Oxalate	Cubic-Y_2O_3	0.5	6.6	1000–5000	Irregular
Y_2O_3	Oxalate	Cubic-Y_2O_3	0.1	4.0	1000–5000	
Y_2O_3	Combustion method	Cubic-Y_2O_3	0.1	4.0	Fractal structure	Sponge-like
Y_2O_3	Polymeric resin	Cubic-Y_2O_3	0.1	1.0	Aggregates of ~10–20	Spheroidal
Y_2O_3	Polymeric resin	Cubic-Y_2O_3	0.5	1.0	Aggregates of ~10–20	Spheroidal
Y_2O_3	Polymeric resin	Cubic-Y_2O_3	6.7	3.3	Aggregates of ~10–20	Spheroidal
Y_2O_3	Polymeric resin	Cubic-Y_2O_3	1.0	1.0	Aggregates of ~10–20	Spheroidal
Y_2O_3	Polymeric resin	Cubic-Y_2O_3	2.0	1.0	Aggregates of ~10–20	Spheroidal
Y_2O_3	Polymeric resin	Cubic-Y_2O_3	3.0	1.0	Aggregates of ~10–20	Spheroidal
Y_2O_3	Polymeric resin	Cubic-Y_2O_3	2.0	1.0	Aggregates of ~10–20	Spheroidal
Y_2O_2S	Polymeric resin	Triclinic- Y_2O_2S	0.1	4.0	Aggreates of 20–30	
Y_2O_2S	Basic carbonate	Triclinic- Y_2O_2S	0.1	4.0	~100	Spherical
Y_2O_2S	Polymeric resin	Triclinic- Y_2O_2S	2.0	1.0	Aggregates of ~20–30	Spheroidal (agglomerate)
La_2O_2S	Commercial standard	Triclinic- La_2O_2S	?	?	2000–5000	Irregular

In Fig. 4, a comparison of the photon ratio of the doped yttrium oxide phosphors with the same average particle size (prepared from the polymeric resin precursor), but different doping ion concentrations is presented. The most efficient oxide upconverters, despite falling in the red region, are the ones that present the higher percentage of Yb^{3+}, corroborating for the data discussed before. Once again, when the percentage of Yb is decreased, there is an increase in the relative intensity of the green counterpart.

In order to compare the upconversion efficiency at the different matrixes, precursors, and doping ion percentage, a graph in Fig. 5 displays representative samples. It is interesting to note that yttrium oxides doped with 0.5 and 6.6% of Er and Yb, respectively, prepared from different precursors (oxalate and polymeric resin) exhibit different behaviors. The oxide prepared from the oxalate precursor, which has particle size in the micron region, is much more efficient than the one prepared from the polymeric resin. In the case of the polymeric resin precursor, particle size is decreased in the order of 15–20 nm, so the decrease in the upconversion efficiency must be related to the nanosized particle effect. This effect due to the decrease in particle size can also be observed when yttrium oxide samples containing 0.1 and 4% of Er and Yb are compared (Fig. 5, samples c, e, f, and g). According to Table 1, the oxide samples with 0.1%Er and 4%Yb present the following diminishing order of particle size as a function of the type of precursor/method: oxalate>combustion method>basic carbonate>polymeric resin. If one analyzes Fig. 5, it is possible to verify that the same samples display a decrease in the upconversion efficiency when the precursor/method is taken into account: oxalate>combustion method>basic carbonate ~ polymeric resin.

The influence of host lattice can be evaluated from Fig. 5 by comparison of the samples (d) and (e), as well as (h) and (g), which contain the same percentage of doping ion but were prepared from basic carbonate and polymeric resin, respectively. The oxysulfide upconverter phosphor has the highest upconversion efficiency when compared to the respective oxide (same doping ion content and similar particle size). The enhancement in the visible upconversion efficiency can be due to differences in multiphonon relaxation rates related to host lattice vibrational modes. Usually, low-phonon energy hosts (such as chloride, bromide and iodide) show stronger upconversion in the visible region than

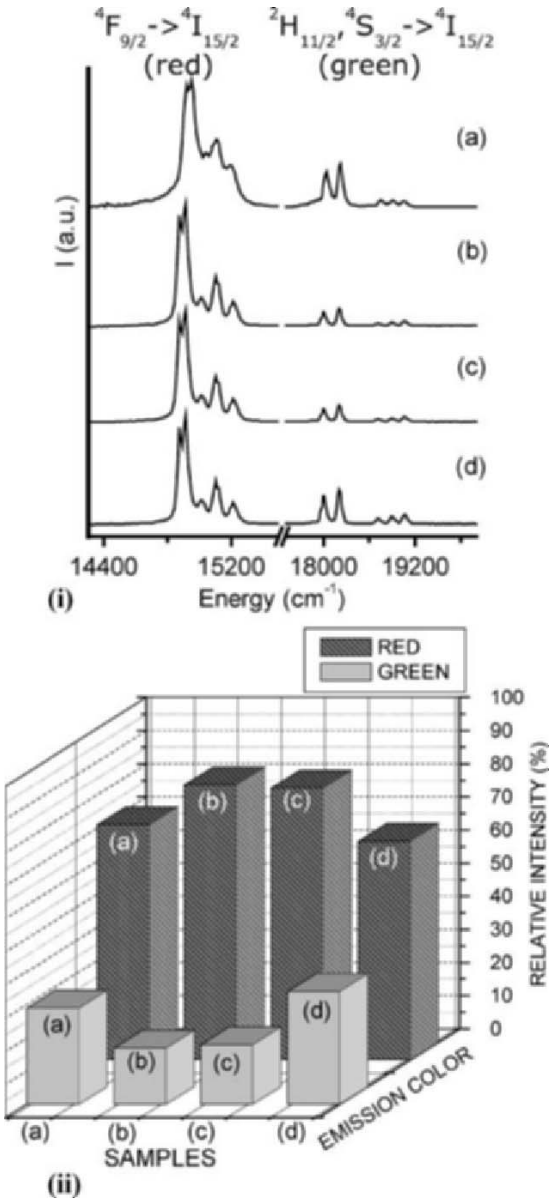

Fig. 2 (i) Emission spectra at room temperature and excitation at 10,212 cm^{-1} for an incident power of 100 mW (unfocused beam) and (ii) comparison of the relative intensity percentage for: (a) Standard Oxysulfide; (b) Y_2O_2S:Er,Yb (0.1%,4%) prepared from basic carbonate; (c) Y_2O_2S:Er,Yb (0.1%,4%) prepared from polymeric resin; (d) Y_2O_2S:Er,Yb (2%,1%) prepared from the polymeric resin

high-phonon-energy hosts (such as oxides and fluorides) [10]. Therefore, the lower phonon energy in yttrium oxysulfide, when compared to yttrium oxide [11], may justify the higher efficiency of upconversion in the visible region in the case of the oxysulfide host.

In Fig. 6, a set of upconversion spectra in the red and green regions is presented in order to illustrate a comparison of the relative intensities of the different samples. From Fig. 6, it is clear how the ratio between the green and red emission

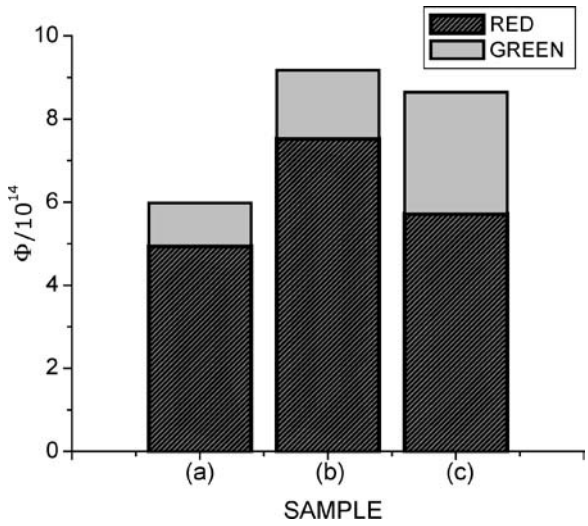

Fig. 3 Comparison of the number of photons (Φ) estimated from emission spectra recorded at room temperature and excitation at 10 212 cm^{-1} for an incident power of 100 mW (unfocused beam): (a) Y_2O_2S:Er,Yb (0.1%,4%) prepared from basic carbonate; (b) Y_2O_2S:Er,Yb (0.1%,4%) prepared from the polymeric resin; (c) Y_2O_2S:Er,Yb (2%,1%) from polymeric resin

SAMPLE	%Er	%Yb
(a)	0.5	6.6
(b)	0.1	4.0
(c)	0.1	1
(d)	0.5	1
(e)	6.7	3.3
(f)	1	1
(g)	2	1
(h)	3	1

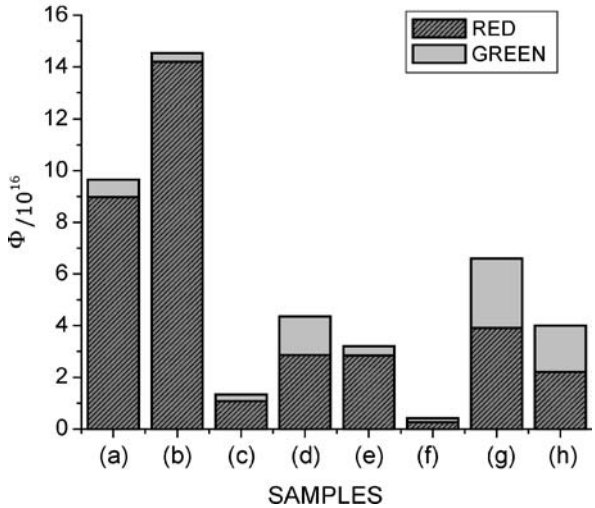

Fig. 4 Comparison of the number of photons (Φ) estimated from emission spectra recorded at room temperature and excitation at 10 240 cm^{-1} for an incident power of 100 mW (focused beam = 50 mm) of the Y_2O_3:Er,Yb samples prepared from the polymeric precursor, but containing different percentages of doping ion

SAMPLE	HOST LATTICE	PRECURSOR	%Er	%Yb
(a)	"	Oxalate	0.5	6.6
(b)	"	Polymeric Resin	0.5	6.6
(c)	Y_2O_3	From Combustion Method	0.1	4.0
(d)	Y_2O_2S	Basic Carbonate	0.1	4.0
(e)	Y_2O_3	Basic Carbonate	0.1	4.0
(f)	"	Oxalate	0.1	4.0
(g)	"	Polymerica Resin	0.1	4.0
(h)	Y_2O_2S	"	0.1	4.0

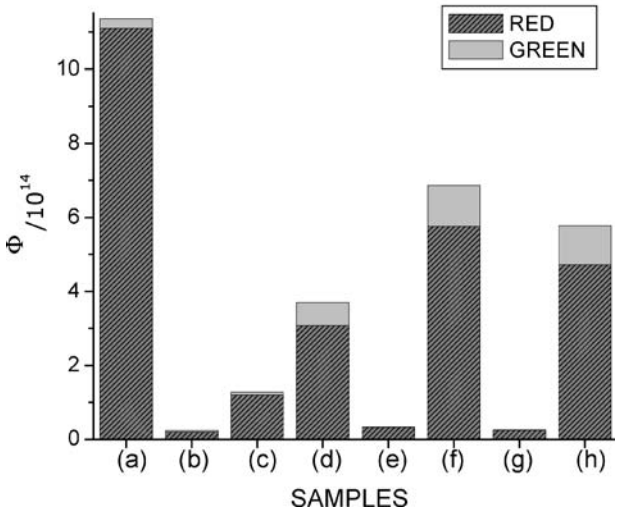

Fig. 5 Comparison of the number of photons (Φ) of the Er,Yb samples, estimated from emission spectra recorded at room temperature and excitation at 10,212 cm^{-1} and 10,240 cm^{-1} for oxysulfide and oxide ones respectively for an incident power of 100 mW (unfocused beam)

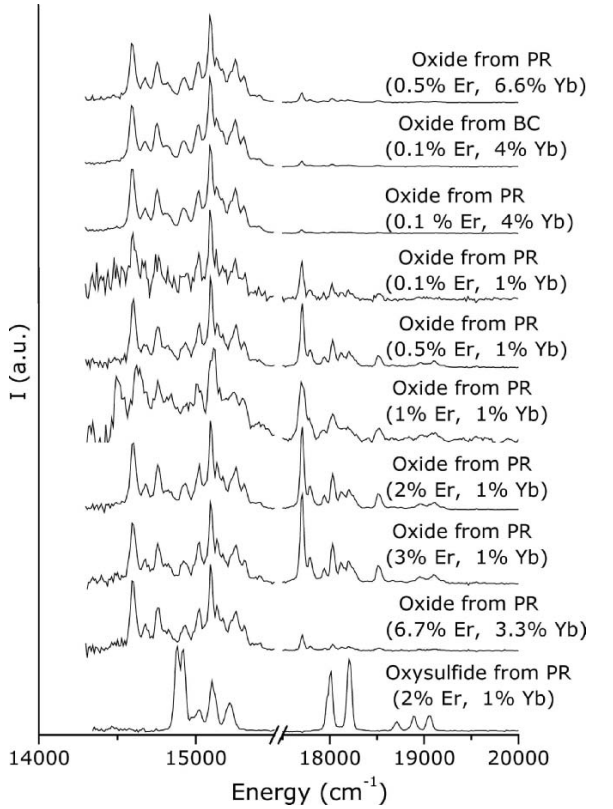

Fig. 6 Emission spectra at room temperature, incident power of 100 mW (focused beam = 50 mm) and excitation at 10,212 cm^{-1} and 10,243 cm^{-1} of upconverter oxysulfide and oxide phosphor samples, respectively, where PR means polymeric precursor and BC means basic carbonate precursor

relative intensities evolve with the variation in the doping ion content.

On the basis of all the results above, it is possible to identify several factors that can rule the light emission behavior of the studied upconverters phosphors. First of all, it is possible to say that, independent of the host lattice, the intensity of the upconversion emission in the visible (green and red) region decreases with decreasing particle size, in agreement with several works reported before, such as [12]. This becomes more evident when phosphors prepared from either the oxalate precursor or from the combustion method are compared to the others, because particle size decreases from micrometers to the nanoscale. However, it is necessary to remember that when phosphors prepared from the polymeric resin and basic carbonate precursors are compared, Fig. 3, the particle size effect is not well observed, because the polymeric resin results in agglomerates of 10–20 nm particles in the case of the oxide host lattice, and 20–30 nm in the case of the oxysulfide host lattice (Table 1). So, as basic carbonate results in monodispersed 90 nm particles, the effect of particle size is much more evident, and in some cases it can be observed that the polymeric resin generates phosphors that are more efficient than similar ones prepared from basic carbonate. Moreover, it was previously reported that yttrium oxysulfide prepared from basic carbonate has a mean crystallite size of 19 nm, and the one obtained from polymeric resin has a size of 18 nm [6]. So, their similar crystallite sizes can also disguise the effect of decreasing particle size. According to Song *et al*. [12], who investigated Y_2O_3:Er,Yb nanosystems, the size dependent upconversion luminescence behavior can be explained by the population of the $^4S_{3/2}/^2H_{11/2}$ Er^{3+} level, where $^4I_{11/2}/^4I_{13/2}$ Er^{3+} non-radiative relaxation processes are involved. The energy gap (ΔE) between $^4I_{11/2}$ and $^4I_{13/2}$ is $\sim$3700 cm^{-1}. For the bulk Y_2O_3 host, the largest phonon energy (*hw*) is only $\sim$600 cm^{-1} [12]. Mikami *et al*. [9] have performed a study of lattice vibrations and optical properties of Y_2O_2S and showed that it presents four Raman-active modes in the range of 140 to 480 cm^{-1} (experimental and theoretical values that are both in agreement). In addition, these authors stated that experimental wavenumbers of the IR modes in Y_2O_2S are not available in the literature, so they only

theoretically predicted eight IR modes in the 200–586 cm^{-1} range. However, da Vila *et al*. 1997 [13], had published the preparation and characterization of uniform, spherical particles of Y_2O_2S and Y_2O_2S:Eu^{3+} using the basic carbonate precursor route, and they reported their IR spectra in both the high frequency region (4000 to 400 cm^{-1}, KBr pellets) and in the low frequency region (1500 to 200 cm^{-1}, Nujol-CsI windows). They also provided a comparison between the experimental IR modes of Y_2O_2S and Y_2O_3. For Y_2O_2S they found four sharp medium bands at 269, 290, 310, and 391 cm^{-1}, as well as one broad and strong band at 467 cm^{-1}. Above this broad band no vibrational modes were detected. For the Y_2O_3 host they observed five sharp bands with weak and strong intensities at 238, 270, 306, 339, and 466 cm^{-1}, as well as two strong broad bands at 380 and 563 cm^{-1}. Therefore, not only in the case of the Raman mode, but also in the case of IR mode, the frequency observed for the Y_2O_3 host is higher that of the Y_2O_2S host. Knowing that the rate of multiphonon relaxation is dominated by $(1 + \langle n \rangle)^P$ (n = phonon density; $P = -\Delta E/hw$), the larger the $\Delta E/hw$, the smaller the rate of multiphonon relaxation [12]. Song *et al*. [12] came to the conclusion that the nonradiative relaxation rate of $^4I_{11/2} \rightarrow {}^4I_{13/2}$ in the bulk Y_2O_3 is relatively small, so it is perfectly possible to apply the same assumption for the Y_2O_2S host. When nanoparticles or small-sized systems are taken into account, the presence of CO_3^{2-} and OH^- groups with high frequency vibrational modes on the surface increases as the particle size decreases. The higher frequencies can induce other norandiative relaxations for Er^{3+}, leading to quenching of the UCL (Upconversion Luminescence).

Secondly, it was possible to confirm that the photons counts of the red emission increases, whereas the green emission one decreases as the concentration of Yb^{3+} increases. This can be observed in both the Y_2O_3 and Y_2O_2S systems, because the dominant mechanism for populating $^4F_{9/2}$ is energy transfer upconversion (ETU) [3, 12]. An increase in the concentration of Yb^{3+} greatly promotes ET from Yb^{3+} ($^3F_{5/2}$) to Er^{3+} ($^4I_{11/2}$), so the $^4F_{9/2} \rightarrow {}^4I_{15/2}$ transition is considerably accelerated because of the increase in the ET process [3, 12].

Concluding remarks

Basically, from the emission spectra collected for efficiency comparisons, it is possible to determine which sample has the most intense emission in the visible region. It is also possible to evaluate how the green and red relative ratios vary in the different samples. In general, independent of the host lattice or particle size, an increase in the percentage of Yb^{3+} results in an increase in the emission intensity, although there is enhancement of the red emission. Probably, there is an increase in the ET from Yb^{3+} ($^2F_{5/2}$) to Er^{3+} ($^4I_{11/2}$), which can play major role in the enhancement of the $^4F_{9/2} \rightarrow {}^4I_{15/2}$ red transition of Er^{3+}. In the case of the oxide samples, when the percentage of Yb^{3+} was kept as 1%, it is possible to observe that the photon counts of the green emission starts to increase, and the number of photons of the total visible emission increases when the percentage of Er^{3+} is increased to 2%. With 3% of Er, the green and red photon ratio is maintained, but the total efficiency decreases, probably because of concentration quenching. So, on the basis of these results, it is possible to choose which system is adequate for a specific assay, considering whether it is more advantageous to have greater contribution from the green or red emissions, or from both in comparable intensities. Although the oxysulfide host lattice results in more efficient phosphors than those containing the oxide lattice (considering similar doping ion content and particle size), the stability of the latter one relative to oxysulfide in oxidative media still make them useful reporters in specific assays.

Acknowledgments AMP and OAS are grateful to FAPESP for financial support.

References

1. Niedbala RS, Feindt H, Kardos K, Vail T, Burton J, Bielska B, Li S, Milunic D, Bourdelle P, Vallejo R (2001) Detection of analytes by immunoassay using up-converting phosphor technology. Anal Biochem 293:22–30
2. Zarling DA, Rossi MJ, Peppers NA, Kane J, Faris GW, Dyer MJ, Gregory San W, Ng SY, Schneider LV (1997) Up-converting reporters for biological and other assays using laser excitation techniques. US patent 5,674,698
3. Pires AM, Serra OA, Davolos MR (2005) Morphological and luminescent studies on nanosized Er, Yb-Yttrium oxide upconverter prepared from different precursors. J Lumin 113:174–182
4. Vetrone F, Boyer JC, Capobianco JA, Speghini A, Bettinelli M (2004) Significance of Yb^{3+} concentration on the upconversion mechanisms in codoped Y_2O_3:Er^{3+},Yb^{3+} nanocrystals. J Appl Phys 96:661–667
5. Pires AM, Heer S, Güdel HU, Serra OA (2005) Low temperature upconversion spectroscopy of nanosized Y_2O_3:Er,Yb phosphor. J Appl Phys 98:063529-1-7
6. Pires AM, Serra OA, Davolos MR (2004) Yttrium oxysulfide nanosized spherical particles doped with Yb and Er or Yb and Tm: efficient materials for up-converting phosphor technology field. J Alloys Compd 374:181–184
7. Dammak M, Maalej R, Kamoun M, Deschanvres JL (2003) Crystal field analysis of erbium doped yttrium oxide thin films in C-2 and C-3i sites. Phys Stat Sol B-Bas Res 239:193–202
8. Tanner PA, Wong KL (2004) Synthesis and spectroscopy of lanthanide ion-doped Y_2O_3. J. Phys. Chem. B 108:136–142
9. Mikami M, Nakamura S (2002) Lattice dynamics and dielectric properties of yttrium oxysulfide. Phys Rev B 65(094302):1–4
10. Gamelin DR, Güdel HU (2000) Upconversion process in transition metal and rare earth metal systems. In: Topics in current chemistry, vol. 214, Springer-Verlag, Berlin Heidelberg

11. Georgobiani AN, Gruzintsev AN, Barthou C, and Benalloul P (2004) Infrared luminescence $Y_2O_2S:Er^{3+}$ andY_2O_3: Er^{3+}. Inorg Mat 40:840–844
12. Song H, Sun B, Wang T, Lu S, Yang L, Chen B, Wang X, Kong X (2004) Three-photon upconversion luminescence phenomenon for the green levels in Er^{3+}/Yb^{3+} codoped cubic nanocrystalline yttria. Sol Stat Commun 132:409–413
13. da Vila LD, Stucchi EB, Davolos MR (1997) Preparation and characterization of uniform, spherical particles of Y_2O_2S and Y_2O_2S:Eu. J Mater Chem 7:2113–2116